Carbohydrate Polymers 94 (2013) 713–722

Contents lists available at SciVerse ScienceDirect

Carbohydrate Polymers

journal homepage: www.elsevier.com/locate/carbpol

Chitosan(PEO)/silica hybrid nanofibers as a potential biomaterial for bone regeneration

Georgios Toskas[a,*], Chokri Cherif[a], Rolf-Dieter Hund[a], Ezzeddine Laourine[a], Boris Mahltig[b], Amir Fahmi[c], Christiane Heinemann[d], Thomas Hanke[d]

[a] Institute of Textile Machinery and High Performance Material Technology (ITM), Technische Universität Dresden, Hohe Str. 6, 01069 Dresden, Germany
[b] University of Applied Sciences, Faculty of Textile and Clothing Technology, Webschulstrasse 31, 41065 Mönchengladbach, Germany
[c] Rhine-Waal University of Applied Sciences, Faculty of Technology and Bionics, Marie-Curie-Straße 1, 47533 Kleve, Germany
[d] Max Bergmann Center of Biomaterials and Institute of Materials Science, Dresden University of Technology, Budapester Str. 27, 01069 Dresden, Germany

ARTICLE INFO

Article history:
Received 29 November 2012
Received in revised form 17 January 2013
Accepted 22 January 2013
Available online 13 February 2013

Keywords:
Chitosan(PEO)/silica nanofibers
Sol–gel
Electrospinning
Cytocompatibility
Bioactivity

ABSTRACT

New hybrid nanofibers prepared with chitosan (CTS), containing a total amount of polyethylene oxide (PEO) down to 3.6 wt.%, and silica precursors were produced by electrospinning. The solution of modified sol–gel particles contained tetraethoxysilane (TEOS) and the organosilane 3-glycidyloxypropyltriethoxysilane (GPTEOS). This is rending stable solution toward gelation and contributing in covalent bonding with chitosan. The fibers encompass advantages of biocompatible polymer template silicate components to form self-assembled core–shell structure of the polymer CTS/PEO encapsulated by the silica. Potential applicability of this hybrid material to bone tissue engineering was studied examining its cellular compatibility and bioactivity. The nanofiber matrices were proved cytocompatible when seeded with bone-forming 7F2-cells, promoting attachment and proliferation over 7 days. These found to enhance a fast apatite formation by incorporation of Ca^{2+} ions and subsequent immersion in modified simulated body fluid (m-SBF). The tunable properties of these hybrid nanofibers can find applications as active biomaterials in bone repair and regeneration.

1. Introduction

Sol–gel derived hybrid silica glass nanocomposite materials and nanofibers have been recently introduced as scaffolding matrices for bone–tissue regeneration (Heinemann et al., 2009; Heinemann, Coradin, Worch, Wiesmann, & Hanke, 2011; Kim, Kim, & Knowles, 2006; Mahony et al., 2010; Poologasundarampillai et al., 2010; Seol, Kim, Kim, & Rhee, 2010). These organic–inorganic nanocomposite materials combine both counterparts in one material, advantaging the flexibility and good mold ability of the organic part, heat-stability, high strength and chemical resistance of the inorganic part. Moreover, coating ability of apatite on ceramics has been known for a long time (Kokubo, 1991) and has been tested on silica glasses of various alkoxide systems (Kim et al., 2006; Poologasundarampillai et al., 2010; Toskas et al., 2011b). The silica hybrid materials favor cell attachment and are not cytotoxic as demonstrated by culture of mesenchymal stem cells (MSCs) on a silica–gelatin hybrid (Mahony et al., 2010), on silica–collagen composites (Heinemann et al., 2009) and that of an osteosarcoma cell line SaOs-2 on a poly(γ-glutamic acid)/silica hybrid (Poologasundarampillai et al., 2010).

Chitosan (CTS) a natural cationic polymer offers unique properties such as biologically renewable, biodegradable, biocompatible, non-antigenic, non-toxic and biofunctional. It is promoting cell adhesion, proliferation and differentiation and evokes a minimal foreign body reaction on implantation (Muzzarelli, 2009). Chitosan with silicate hybrids were synthesized with glycidoxypropyltrimethoxy silane (GPTMS), whose epoxy groups are considered to react with the amino groups of chitosan. The cross-linking density was around 80% regardless of the amount of silane (Muzzarelli, 2011). The values of the mechanical parameters indicated that significant stiffening of the hybrids was obtained upon addition of the silane while full flexibility was retained. In addition, adhesion and proliferation of the MG63 osteoblast cells cultured on the hybrid surface were improved compared to those on the pure chitosan membrane regardless of the silane concentration (Muzzarelli, 2011; Shirosaki et al., 2005; Shirosaki, Botelho, Lopes, & Santos, 2009a). MC3T3-E1 cells also showed comparable viability on sol–gel derived silica xerogel/chitosan hybrid coatings onto alkali-treated titanium, proving their potential to be used as

* Corresponding author. Present address: Technological Education Institute of Piraeus, School of Engineering, Department of Textiles, 250 Thivon & P. Ralli, 12244 Egaleo, Greece. Tel.: +30 210 5381171/5381333; fax: +30 210 5381255.
E-mail addresses: georg.toskas@gmx.de, gtoskas@gmail.com (G. Toskas).

0144-8617/$ – see front matter © 2013 Elsevier Ltd. All rights reserved.
http://dx.doi.org/10.1016/j.carbpol.2013.01.068

bioactive coating materials in hard tissue engineering (Jun et al., 2010). Moreover chitosan was found to improve structural integrity of PEO cross-linked by silicate nanoparticles (Laponite) films and to enhance the formation of a mineralized extracellular matrix and the differentiation of MC3T3-E1 preosteoblast cells (Gaharwar, Schexnailder, Jin, Wu, & Schmidt, 2010).

Glass ceramic silica (SiO_2) electrospun nanofibers have received significant attention due to their multifunctional properties in biomedical fields (Kim et al., 2006; Seol et al., 2010; Sridhar, Sundarrajan, Venugopal, Ravichandran, & Ramakrishna, 2012). There are two main methods of preparing silica electrospun nanofibers via solutions (spin dopes): the first is by the direct spinning from aged sol–gel solutions containing alkoxide precursors; the second involves carrying polymers and is more advantageous as it can be easily adjusted, generating nanofibers of controllable size and uniformity. As alkoxide precursor, tetraethoxysilane (TEOS) and tetramethoxysilane (TMOS) are commonly used (Choi, Lee, Im, Kim, & Joo, 2003; Shao et al., 2003). As carrying co-electrospun homopolymer polyvinyl pyrrolidone (PVP), polyvinylidene fluoride (PVDF), nylon-6 and polyvinyl alcohol (PVA) are common studied polymers (Gaharwar et al., 2010; Kim, Ahn, & Choi, 2010; Liu et al., 2008; Shao et al., 2003). Recently, new types of organic–inorganic silica nanofibrous (SiO_2) composite membranes developed based on one of the most frequently used non-toxic and biocompatible polymers, polyethylene oxide (PEO) (Toskas et al., 2011b). A new organically modified alkoxide sol–gel solution was used containing a mixture of tetraethoxysilane (TEOS) and 3-glycidyloxypropyltriethoxysilane (GPTEOS). Organosilanes such as GPTEOS are having the advantage of bearing organic and inorganic functionalities in the one molecule which provide the ability to bond to organic chains and inorganic moieties accordingly. Moreover, major advantage of this combined alkoxide sol–gel precursor is to increase the stability of GPTEOS toward gelation up to several months (Mahltig, Fiedler, Fischer, & Simon, 2010). It is also suggested that organosilanes as γ-glycidoxypropyltrimethoxy silane (GPTMS) slow condensation reaction rate and enhance the polymer–silica compatibility (Liu, Su, & Lai, 2004).

Chitosan (CTS) nanofibers via electrospinning were first obtained from neat trifluoroacetic acid (TFA) at 7 wt.% (Ohkawa, Cha, Kim, Nishida, & Yamamoto, 2004). But the more usual method involves the use of polyethylene oxide (PEO) as co-blending polymer, in order to spin chitosan at higher polymer concentrations (Bhattarai, Edmondson, Veiseh, Matsen, & Zhang, 2005; Klossner, Queen, Coughlin, & Krause, 2008; Toskas, Laourine, Kaeosombon, & Cherif, 2009). Combining the unique collective properties of both materials, the fabrication of composite organic–inorganic CTS/SiO_2 nanofibers via electrospinning is of great interest. Introduction of silica into biomaterials was early proved to increase its oxygen permeability, biocompatibility, and biodegradability (Suzuki & Mizushima, 1997; Tian et al., 1997). In this work, a controllable process of creating CTS(PEO)/SiO_2 nanofibers is presented; the effect of varying the polymer to silica precursor weight ratio is examined and correlated to the structural properties of the nanofibers. Subsequently, the ability of these hybrid nanofibers to favor cell attachment of 7F2 osteoblasts is tested and also their capability to modify by incorporating calcium ions resulting in bioactive hydroxyl carbonate apatite (HCA) crystal formation were in parallel examined.

2. Materials and methods

2.1. Materials

Chitosan from crab shells with >75% of deacetylation (M_W = 200 kD) and polyethylene oxide (PEO) (M_W = 900 kD) were obtained from Sigma, Germany. Acetic acid was bought from Normapur (PROLABO), Germany. Deionized water was used for the preparation of solutions. Dulbecco's Modified Eagle's Medium (DMEM—D6046)—low glucose with 1000 mg/L glucose, L-glutamine and sodium bicarbonate, liquid sterile filtered was also purchased from Sigma, Germany.

2.2. Preparation of electrospun nanofibers

The modified silica sol was prepared by hydrolyzing tetraethoxysilane and 3-glycidyloxypropyltriethoxysilane in a weight ratio of 3:1. The sol was hydrolyzed in 0.01 N HNO_3 and in presence of ethanol, in a volume ratio of: (TEOS/GPTEOS):HNO_3:C_2H_5OH = 1:0.2:4.2. After stirring for 24 h, the solution was ready for the preparation of the spin-dopes. A 3 wt.% PEO solution was prepared separately in 0.5 M acetic acid and stirred for a period of 24 h. Then, 2.5 wt.% of chitosan (CTS) solution and 3.0% PEO solution in acetic acid were blended with variable weight ratios of chitosan to PEO. The optima results as to nanofibers production were obtained at a chitosan/PEO ratio of 60:40 with 20 wt.% total acetic acid concentration. This ratio was kept stable for the mixed chitosan(PEO)/silica solutions. Afterwards, the CTS(PEO) solutions were mixed in various weight ratios with the alkoxide solution. The resultant mixtures were stirred for at least 6 h to ensure adequate mixing.

The electrospinning apparatus was set up horizontally, as it has been previously described (Toskas et al., 2011a). The silica/polymer solution was put into a 1 mL disposable syringe fitted with 0.60–1.0 mm 23 gauge tip-ground-to-flat needles and fed with the help of a programmable KD scientific pump. The ambient conditions occurred at temperatures of 20–22 °C and 50–55% RH. Typical parameters operated in this study were flow rates between 0.4 and 1.0 mL/h, voltages between 25 and 28 kV and a tip to collector optimal distance of 11 cm.

2.3. Characterization

2.3.1. Rheology

A Haake MARS (Haake, Germany) stress-controlled rheometer was used for the measurements of the solutions viscosity parameters. Cone-plate geometry (35 mm radius, 2°, Ti) was used for the shear measurements and the oscillatory movement. The gap for all solutions was 0.100 mm at a temperature of 20 ± 0.1 °C.

2.3.2. Microscopy: scanning electron microscopy-EDX, transmission electron microscopy, fluorescence microscopic images

A DSM 982 Gemini (Zeiss, Germany) Scanning Electron Microscope served for the examination of the morphology of the nanofibers. The as-spun nanofibers were dried under vacuum at room temperature and sputter-coated with silver/graphite. The samples were examined at an accelerating voltage of 1.0 kV and magnifications from 200 to 50,000. The SEM images were then used to evaluate the fiber diameter. The average fiber diameter was determined using Digital Image Processing System 2.6 (point electronic GmbH) software in conjunction with the SEM image. Ten different fiber diameters were determined and averaged to find the fiber diameter reported for each of the resulting electrospun mats. The 95% confidence limits of the mean were calculated and reported with each average fiber diameter.

For the transmission electron microscopy (TEM), the samples were deposited as received in copper TEM grids carbon-coated copper grids (400 meshes, AGAR Scientific). Transmission electron microscope (TEM) from TECNAI Biotwin (FEI Ltd.) at 100 keV was used to observe the samples. Any treatment has been performed on the microfibers to avoid any deterioration of the samples.

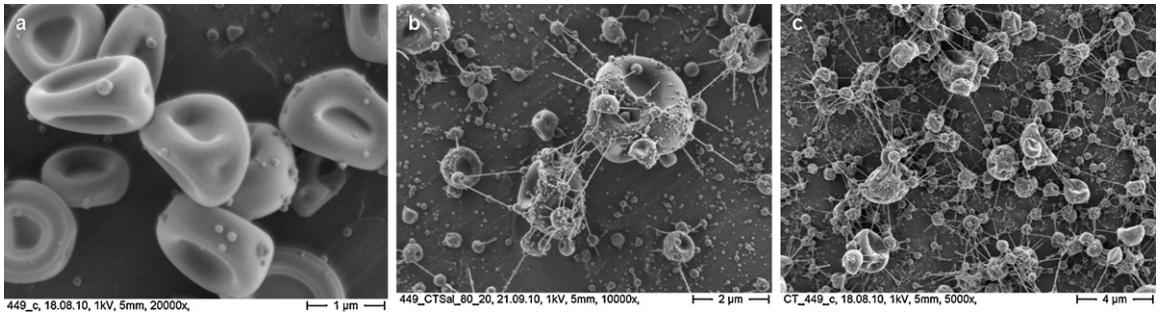

Fig. 1. Electrosprayed TEOS/GPTEOS spin dope (a) and electrospinning attempts of 2.5 wt.% CTS/SiO_2 ((b) magnification 10,000×, (c) magnification 5000×).

Fluorescence microscopic images have been taken with a Zeiss Axioskop 2 FS mot equipped with both a Zeiss Plan Neofluar® 10×/0.3 and a Zeiss Plan-Apochromat® 20×/0.75. The excitation was performed by a 50 W-mercury lamp. Filter sets Zeiss Nr 1 (DAPI) as well as Zeiss Nr. 9 (Alexa Fluor 488®) have been used.

2.3.3. Infrared spectroscopy

IR spectra were obtained by using the attenuated total reflection (ATR) method on a FTIR Bruker Tensor 27 spectrophotometer.

2.3.4. Cell culture and staining

Nanofibrous membranes for cell culture were prepared on titanium plates (10 mm diameter) by dip coating. After coating, drying at 37 °C and 20% relative humidity was performed over 24 h in a climate chamber. The resulting membranes on titanium plates were sterilized by gamma-irradiation (25 kGy) before starting the cell culture experiments. Murine osteoblast-like cell line 7F2 was obtained from the American type Culture Collection (ATCC). Cells were expanded in minimal essential medium (R-MEM) supplemented with 10% fetal calf serum (FCS), 2 mM L-glutamine, and the antibiotics penicillin (100 U/mL) and streptomycin (100 U/mL) in a humidified atmosphere (37 °C, 7% CO_2). Medium and all supplements were obtained from Biochrom, Germany.

The membranes were placed in 48-well plates and soaked in cell culture medium for 24 h. After removing the medium, 40 μL of cell suspension (2500 cells μL) was placed onto each sample. Cells were allowed to adhere for 30 min in the incubator before filling up the wells with additional medium. The medium was changed every second day.

In order to evaluate cell morphology, spreading, and growth using fluorescence microscopy actin cytoskeleton as well as the nuclei were stained after 1 day and 6 days. To that end, after washing and fixing, the cells were permeabilized with 0.2% Triton-X-100 in PBS and blocked with 1% bovine serum albumin (BSA, Sigma) for 30 min. Cytoskeletal actin was stained with AlexaFluor 488-Phalloidin (Invitrogen), and cell nuclei were stained with 4′,6-diamidino-2-phenylindole (DAPI, Sigma).

2.3.5. Bioactivity test

For the development of apatite nucleation sites on the hybrid silicate nanofibers, CaO in the form of calcium chloride dihydrate was added in the initial sol–gel solution, before electrospinning. The molar ratios of $CaCl_2{\bullet}2H_2O$, GPTEOS, TEOS, ethanol, HNO_3 and water were 0.08:0.2:0.6:13.5:0.004:1.9, respectively. The bioactivity of the as-obtained nanofibers was assessed for their apatite forming ability in modified simulated body fluid (m-SBF) according to Oyane et al. (2002) (see the Supporting Information, Table 1). The specimens of 10 mg were placed in a Petri glass disk and immersed in 10 mL of m-SBF solution buffered at pH 7.4 for up to 7 days without refreshing. Temperature was held at 37 °C through gentle stirring. After soaking, the samples were carefully rinsed with deionized water, and dried at room temperature.

3. Results and discussion

3.1. Synthesis and properties of spin dopes—morphology and structure of CTS(PEO)/SiO_2 nanofibers

The organically modified alkoxide sol–gel solution containing the mixture of silanes tetraethoxysilane (TEOS) and 3-glycidyloxypropyltriethoxysilane (GPTEOS) in a weight ratio of 3:1 was prepared for electrospin. No alteration on the gelation of this combined alkoxide sol–gel precursor over time was observed up to several months due to the increased stability of GPTEOS (Mahltig et al., 2010). Electrospinning of the silane solution itself, designated hereafter as SiO_2, presenting a dynamic viscosity of only 5 mPa s, resulted in nanodroplets through electrospraying (see Fig. 1a). Also, electrospinning attempts with pristine chitosan (2.5 wt.% CTS) in mixture with the sol–gel solution in various ratios, were not effective leading to bead formation. Beads possess the same form as these produced by the precursor of silica alone, but interconnected with nanofibrils (see Fig. 1b and c). Strong electrostatic forces are suggested in the origin of this micro- and nano-particle formation (Coradin & Livage, 2007; Coradin, Durupthy, & Livage, 2002). The attractive force through the electrostatic interactions between the positively charged ammonium groups of the chitosan backbone and the negatively charged poly(silicic acid) $[SiO_x(OH)_{4-2x}]_n$ oligomers favors their condensation, inducing silica precipitation (Coradin & Livage, 2007). The addition of polyethylene oxide (PEO) was proved essential to obtain a successful electrospinning. PEO containing neutral moieties reduces the chitosan solution viscosity relaxing chitosan chain entanglement. Besides, the possible interaction between PEO and the sol–gel alkoxide is considered through hydrogen bonds. According to our hypothesis, PEO could intercalate in between the positively charged chitosan and the negatively charged silicates. In this model, PEO minimizes the reactivity of silicates and allows dispersion of the two phases preventing direct deposition of silicates as beads during electrospinning.

Chitosan (CTS) is successfully electrospun with PEO as co-blending polymer in various ratios. The polymer system consisting of 2.5 wt.% of chitosan (CTS) solution and 3.0 wt.% PEO solution in acetic acid by weight ratio of 60/40, the ultimate aim is to obtain the optima results as to the CTS/PEO nanofiber uniformity and repetitiveness of process (see the Supporting Information, Fig. SF-1) (Toskas, Hund, Laourine, & Cherif, 2012). Subsequently, varied the weight ratio between the polymer (CTS/PEO 60/40) to alkoxide (TEOS/GPTEOS 3/1) solution in order to reveal a composition window in which uniform nanofibers could be generated.

Critical chain entanglement among the macromolecular chains is related to the electrospinning ability of a polymer solution. The

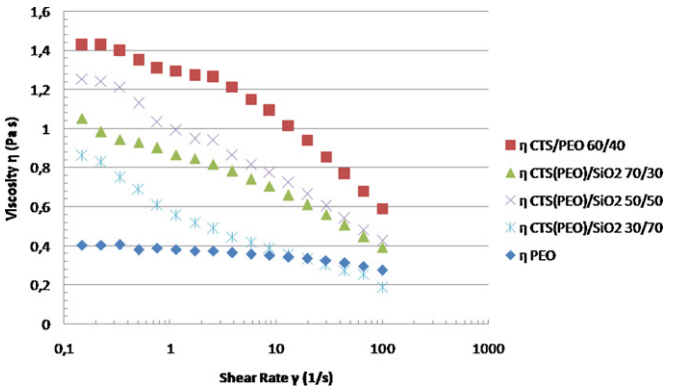

Fig. 2. Shear viscosity as a function of shear rate of various polymer/silica blends of CTS(PEO)/SiO_2 compared to 3.0 wt.% PEO alone and CTS/PEO 60/40.

viscosity of these solutions is an expression of the intermolecular interactions among the polymer chains. First, the effect of the interactions of polymer CTS(PEO) content in the mixed sol–gel solution was examined. This would affect the viscosity and thus the spinnability of solutions. The shear viscosity as a function of shear rate was measured for solutions of different CTS(PEO)/SiO_2 ratios as shown in Fig. 2. The initial dynamic viscosity of 3.0 wt.% PEO was measured 0.407 Pa s, whereas weight ratio of CTS/PEO 60/40 giving uniform nanofibers with diameters down to 40 nm was found 1.44 Pa s. Dynamic viscosities of mixtures CTS(PEO)/SiO_2 ranged in between the above mentioned values: 0.86 Pa s for the CTS(PEO)/SiO_2 30/70 wt. and 1.25 Pa s for the ratio 50/50 wt.% (see Fig. 2). The images of the corresponding as-spun CTS(PEO)/SiO_2 and CTS/PEO nanofibers are shown in Fig. 4 and Fig. SF-1.

The diagram in Fig. 2 shows that the viscosity of the CTS(PEO)/SiO_2 blends decreased monotonically with decreasing polymer content. Nevertheless, the curve of the CTS(PEO)/SiO_2 50/50 wt.% ratio superposes that of 70/30 wt.% ratio. This is suggested due to stronger intermolecular interactions among the polymer chains and the silicon alkoxide network. In fact, other rheological factors such as elastic modulus (G') and loss modulus (G'') are playing significant role in enhancing chain entanglement. In the spin experimental dopes, it was found that the loss modulus G″ is dominating the elastic modulus G' ($G'' > G'$) at low frequencies (see in Supporting Information, Fig. SF-2). This is a typical behavior for an entangled solution. Moreover, for the CTS(PEO)/SiO_2 70/30 wt.% ratio, a crossover occurs ($G'' = G' = 70.9$ Pa) at 9.4 Hz and from that point on at higher frequencies, the elastic modulus (G') dominates G'' (Fig. SF-2c). On the contrary for the CTS(PEO)/SiO_2 50/50 wt.% ratio, the crossover observed at $G'' = G' = 16.13$ Pa has shifted to a lower frequency of 5.45 Hz (Fig. SF-2d). This shift of the crossover point has been correlated with the effective cross-linking change or chain entanglement (Chronakis & Ramzi, 2002). Strong hydrogen bonding between the silicate and CTS(PEO) polymer chains are formed. Furthermore, covalent bonds involving the epoxy group of the silane GPTEOS are considered to be at the origin of this enhanced entanglement.

Uniform nanofibers with smooth surface were obtained within a composition window of CTS(PEO)/SiO_2 ranging from 70/30 to 20/80 wt.% ratios (see Fig. 3). Spinning conditions as voltage, temperature and relative humidity were kept fixed so that only the polymer/solvent and silica oxide properties could influence the fiber morphology. The average diameters of the as-spun nanofibers are increasing from 239 ± 13 nm for the CTS(PEO)/SiO_2 70/30 wt.% ratio to 508 ± 62 nm for the 30/70. The CTS(PEO)/SiO_2 50/50 wt.% ratio presents the smaller average diameter rating 182 ± 16 nm (see Fig. 4). This finding is in good agreement with the rheological results discussed above, provoking a tighter entanglement of the chains (Fig. 2). The CTS(PEO)/SiO_2 70/30 wt.% electrospun nanofibers present a "sticky" surface and are interconnected as the CTS/PEO 60/40 wt.% electrospun alone (see Supporting Information, Fig. SF-1a and b). When introducing over 80% in wt.% of the silica component fibers become less uniform with a large diameter distribution ranging from 866 to 249 nm. Then, over a CTS(PEO)/SiO_2 10/90 wt.% ratio beads appear within the non-uniform nanofiber network. The minimum amount of carrying polymers required for the continuous fiber production via electrospinning is found to 4.5 wt.% CTS and 3.6 wt.% PEO correspondingly. Compared with the average nanofiber diameter of CTS/PEO 60/40 wt.% of 88 ± 15 nm, the nanofiber diameters measured with the silica blend systems are about 2–5 times enlarged by increasing the silica content. These are found also higher in average diameter compared with pristine PEO nanofibers measured 151 ± 23 nm. An enhanced compact structure is resulted by chitosan due to a stronger interaction among silicate and CTS(PEO) polymer chains. The investigated formulation showed also an excellent electrospinnability when a rotating collector with a 4 mm diameter was used. At a rotational speed of 200 rpm, a solution of CTS(PEO)/SiO_2 30/70 wt.% produced a thick nanofiber mat. The nanofibers produced with this method presented also smooth surfaces and possessed a smaller average diameter of 339 ± 65 nm (see in Supporting Information, Fig. SF-3). It is worth to mention that silicon is detected by EDX on the fiber surface of all samples (Supporting Information, Fig. SF-3, insert).

Transmission electron microscopy (TEM) permitted to identify the inner morphology of the nanofibers. The micrographs demonstrate that the nanofibers are composed of compact aligned dots encapsulated by the other material in a core–shell structure (Fig. 5). The differences in contrast along the nanofibers show dark dots having the form of elongated capsules indicated by red circles in Fig. 5a and b and in more detail in Supporting Information, Fig. SF-4a and b. This effect is observed to CTS(PEO)/SiO_2 ratios of 50/50 and 30/70 wt.% whereas increasing the amount of silica in the system stretched the capsules within the fibers. With the ratio CTS(PEO)/SiO_2 of 10/90 wt.% where the relative polymer mass is much inferior to the silicate component, these capsules are stretched to form a uniform core fiber (indicated by a red arrow in Fig. 5c and in more detail in Supporting Information, Fig. SF-4c). As confirmed by EDX and mainly by ATR–FTIR analysis (Supporting Information, Fig. SF-3 and Fig. 6), silicon was always detected on the fiber surface. This finding suggests that the external coating is consisted of the silicate component, chitosan/PEO being incorporated as a core material in self assembled hybrid nanofibers' structures. A complex phase separation occur leading to organic polymer inclusion. The formation of core–shell structure in various polymer–polymer–solvent systems has been attributed to factors that include the different solubility of the two components, variations in rheological parameters, diverse in the blending ratio molecular weight of the polymers and temperature (Wei, Lee, Kang, & Mead, 2005; Zhang et al., 2009). The binodal phase separation of the ternary system by nucleation and growth, assisted by the stronger mobility of chitosan polymer chains induced by acetic acid, seems more likely ascribe to the core–shell structure of our system. This hypothesis is based on the consideration that CTS/PEO is a homogenously behaving polymer system. Actually, no phase separation is observed in nanofibers obtained by CTS/PEO 60/40 wt.% electrospun alone (see the Supporting Information, Fig. SF-1c). For CTS(PEO)/SiO_2 hybrids, solvent surface tension and removal of the solvent during electrospinning process plays an important role in the core–shell formation. In fact, electrospinnability of this hybrid system is influenced by the solution surface tension. It is lowered by the addition of the alkoxide solution containing about 87% w/v ethanol (surface tension $\gamma = 22.3$ mN/m) to the aqueous CTS/PEO solution (~80% (w/v) H_2O $\gamma = 72$ mN/m; (~20% (w/v) CH_3COOH $\gamma = 27.6$ mN/m). Hence, ethanol is more rapidly evaporated

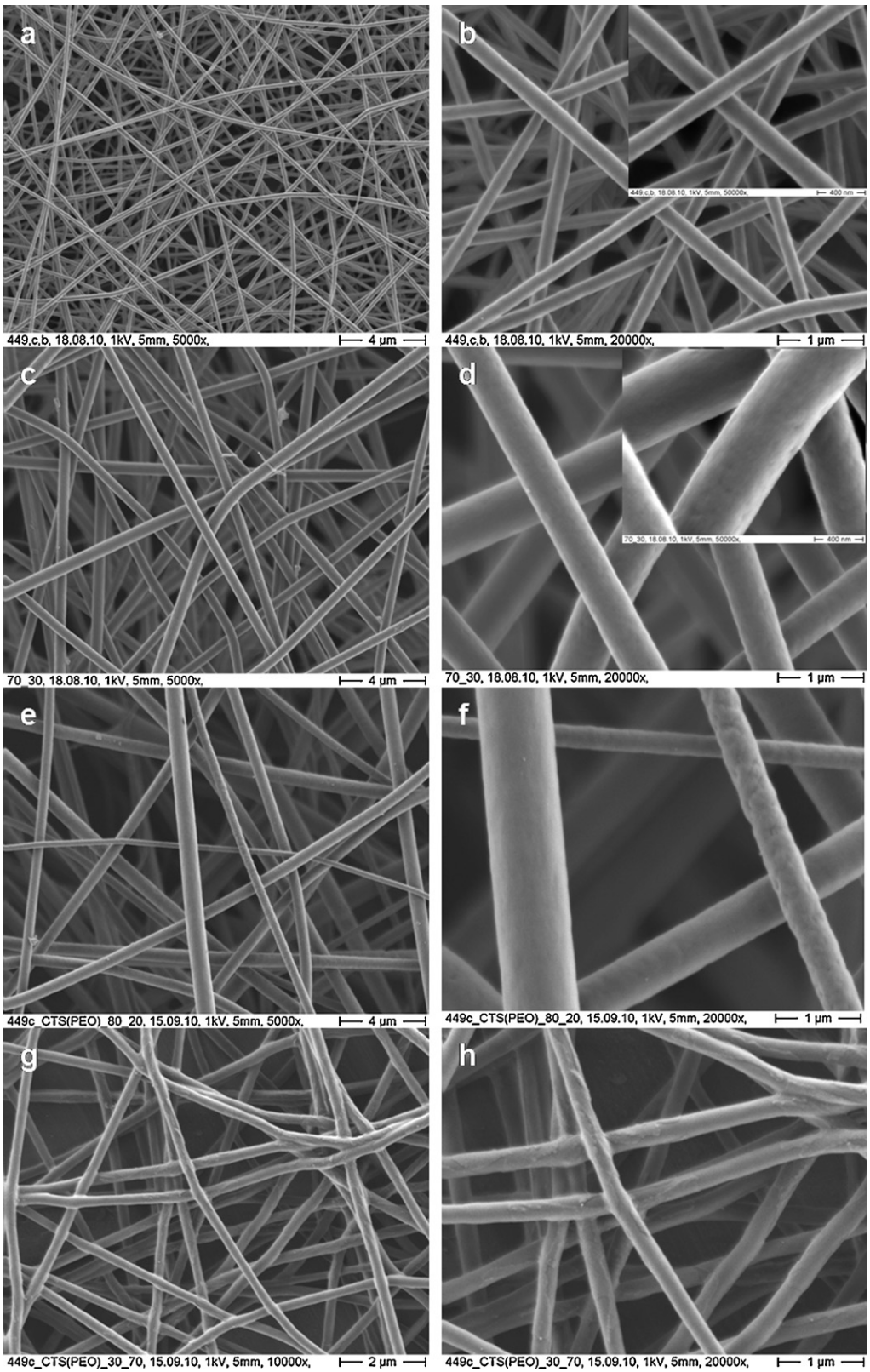

Fig. 3. CTS(PEO)/SiO_2 electrospun nanofibers from 50/50 wt.% ratio ((a) magnification 5000×, (b) magnification of 20,000×; inset: magnification 50,000×), 30/70 weight ratio ((c) magnification 5000×, (d) magnification 20,000×; inset: magnification 50,000×), 20/80 ((e) magnification 5000×, (f) magnification 20,000×) and 70/30 wt.% ratios ((g) magnification 10,000×, (f) magnification 20,000×).

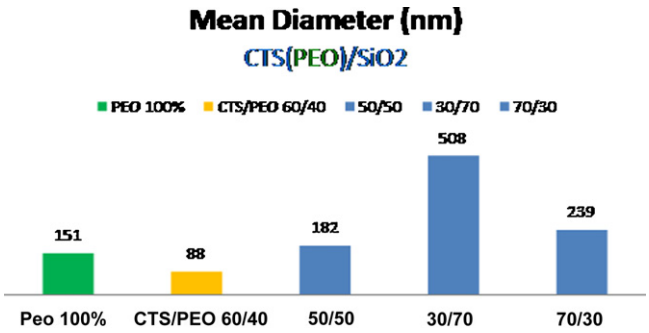

Fig. 4. Effect of polymer (CTS(PEO)) weight ratio on fiber diameter.

during electrospinning, decreasing temperature at the fiber surface. This reduction of temperature varying for the two components, can lead to a thermally induced phase separation of silicate and CTS/PEO, inducing diverse free energy surfaces and resulting in self assembled core–shell structures.

3.2. Composition and integrity of the hybrid nanofibers

The interactions of the hybrid fibers compositions were confirmed by ATR–FTIR spectra. Fig. SF-5a in Supporting Information is presenting the FTIR spectrum of the TEOS/GPTEOS (designated as SiO_2) nanoparticles electrosprayed from the initial alkoxide solution. The characteristic bands of silica xerogel are observed: at 1078 cm^{-1} and 950 cm^{-1}, 795 cm^{-1} are assigned to Si—O—Si and Si—OH stretching vibrations, respectively (Allo, Rizkalla, & Mequanint, 2010). The wide peak in the range 3300–3700 cm^{-1} is assigned to the hydroxyl stretching of the silanol groups. In the stronger peak of 1078 cm^{-1} a shoulder at about 1192 cm^{-1} is attributed to the presence of epoxy group from the 3-glycidyloxypropyltriethoxysilane while a smaller peak at about 2840 cm^{-1} can be attributed to the ethoxy group (—OCH_2CH_3). The ATR–FTIR spectrum of CTS/PEO electrospun nanofibers is demonstrated in Fig. SF-5b. The wide peak at 3300–3700 cm^{-1} is assigned to the stretching of the CTS hydroxyl groups. The medium band at 2889 cm^{-1} and the strong triplet band at 1147 cm^{-1}, 1104 cm^{-1} and 1064 cm^{-1} with a maximum at 1104 cm^{-1} are attributed to the C—H stretch and C—O—C accordingly of the PEO. The bands assigned to the C—H wagging at 1343 cm^{-1}, C—H twist at 1280 cm^{-1} and C—H rocking at 961 cm^{-1} and 848 cm^{-1} are also observed. In the same spectrum (Fig. SF-5b), the carbonyl, C=O—NHR absorption band was observed at 1653 cm^{-1} and the amine —NH_2 absorption band at 1560 cm^{-1}, respectively. These are characteristic of chitosan and are denoted as amide I and II, respectively (Shirosaki et al., 2009b).

ATR–FTIR spectra of CTS(PEO)/SiO_2 nanofibers of various ratios are shown in Fig. 6. All of these spectra resemble that of alkoxide alone (Fig. SF-5a). The GPTEOS-containing hybrids showed ν(Si—O) bands in the 1110–1000 cm^{-1} region. The Si—O—Si stretching assignment of silica at 1078 cm^{-1} is superposed with the strong peak of PEO assigned to C—O—C stretching at 1104 cm^{-1} and has shifted to lower wavelengths with a maximum of around 1065 cm^{-1}. The medium secondary shoulder band at about 1192 cm^{-1} indicates the presence of an epoxy group from the 3-glycidyloxypropyltriethoxysilane. The silane assignments at about 940 cm^{-1} and 793 cm^{-1} ascribed to the Si—O—Si and Si—OH stretching vibrations related to the surface of SiO_2, are also present. The amide I and II bands of chitosan at 1650 and 1565 cm^{-1} respectively are much weaker but still present, except when the SiO_2 content is higher than 80 wt.% (Fig. 6d). Besides, the weak band at 2875 cm^{-1} probably results from the ethoxy groups of GPTEOS, the broad band at 3275–3244 cm^{-1} indicating that most of the ethoxy groups are hydrolyzed to silanol groups (Si—OH). These hydroxyl groups are considered on the electrospun silicate component surface. These findings corroborate our hypothesis that new compact self-assembled hybrid nanofibers are formed.

Moreover, it is likely that a certain fraction of GPTEOS in the hybrid is linked via the epoxy group to chitosan. First, the hydrolyzation and condensation of GPTEOS with TEOS molecules give rise to Si—O—Si bridging oxygen and yield silanol groups (Si—OH). The organosilane formed, conduct organic and inorganic domains in the same molecule (see 1st step in Scheme 1). Simultaneously, GPTEOS could be functionalized through nucleophilic attack to the most substituted carbon of the oxirane, which forms the most stable carbocation. This reaction can catalyzed by the acetic acid and lead to ring opening of the epoxy group. As to the possible interactions between chitosan and the epoxy group of alkoxide, different approaches have been yet proposed. According to Liu et al. (2004), a direct acid-catalyzed amino-oxirane addition reaction, cross-linking —NH_2 to —CH_3 end unit of the ring, is taking place. Unlike to this mechanism, Spirk et al. (2012) have recently considered that covalent bonds between silanes and chitosan can only proceed via the hydroxyl groups of chitosan (see 2nd step (a) in Scheme 1), due to the formation of strong Si—O bonds (av. 440 kcal mol^{-1}) rather than weaker Si—N bonds (av. 0 kcal mol^{-1}). We consider that an ionic bond between the under acidic conditions (pH 3.0) protonated amine groups (—NH_3) of chitosan and the negatively charged esterified oxygen, resulting of the epoxy group, is possible. Besides, an addition copolymerization, implicating the chitosan amine groups and GPTEOS/TEOS silane carbonyls of the esterified ends and resulting in amide synthesis with methanol as by-product, is much feasible (see 2nd step (b) in Scheme 1). In any case, covalent bonds are most likely to be present into the matrix together with hydrogen bonds (Poologasundarampillai et al., 2010). Further quantification is under way in order to unveil the bridging configurations of this complex system.

For applications such as tissue repair and regeneration, mechanical integrity of the scaffolds is critical in order to support cell attachment, differentiation and growth. Chitosan does not dissolve in water under near neutral conditions. On the contrary, PEO has

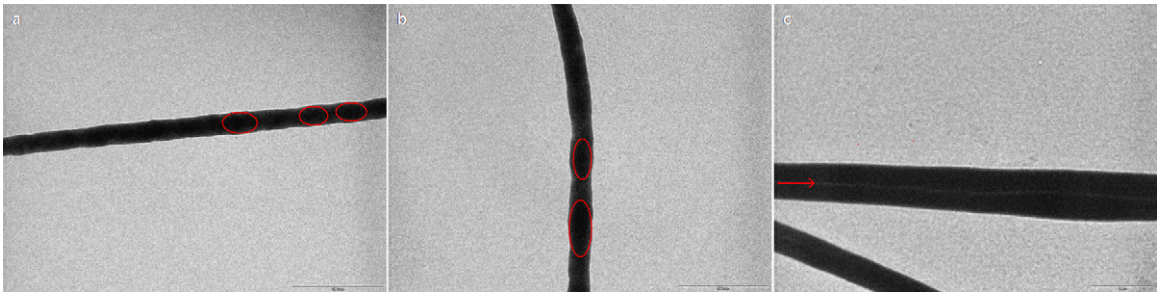

Fig. 5. TEM micrographs of CTS(PEO)/SiO_2 in various ratios revealing the core–shell structure: (a) 50/50, (b) 30/70 and (c) 10/90.

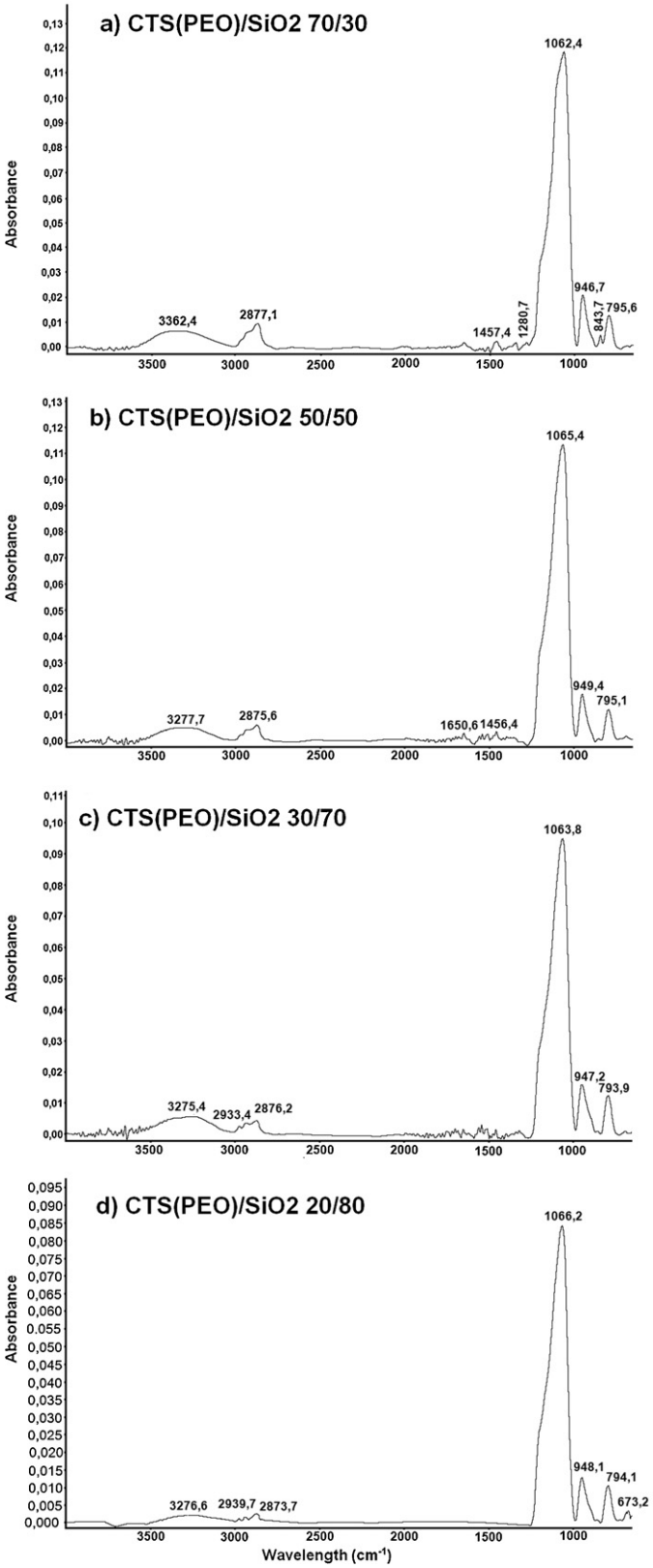

Fig. 6. ATR–FTIR spectra of CTS(PEO)/SiO_2 nanofibers of various ratios (a) 70/30, (b) 50/50, (c) 30/70 and (d) 20/80.

a high solubility in water, and electrospun pure PEO fibrous membranes dissolve readily in water at 37 °C. We have examined the integrity of the hybrid CTS(PEO)/SiO_2 nanofibers in deionized water at 37 °C after immersing 1 day and 6 days. After 1 day of immersion, the nanofibers remain intact. The CTS(PEO)/SiO_2 nanofibers with ratio 30/70 wt.% present rougher surfaces (see in Supporting Information, Fig. SF-6a and b, upper panel). A contraction of 27% is measured for the 30/70 wt.% ratio nanofibers while only a small decrease of 1.2% is observed for the 50/50 wt.% ratio nanofibers. After 7 days immersion, the nanofibers of CTS(PEO)/SiO_2 30/70 wt.% ratio retain their integrity in water and morphology, although they show a slight swelling (Fig. SF-6d, lower panel). The nanofibers of CTS(PEO)/SiO_2 50/50 wt.% ratio although they retain their initial fibrous structure, present a first stage of polymer (probably PEO) release, eventually caused by acetic acid remaining traces (Fig. SF-6c).

Pyrolysis is usually applied in polymer/silica systems in order to eliminate the carrying polymer from the nanofibers. Chitosan does not melt but degrade at a temperature higher of 313 °C, according to the degree of deacetylation (Agboh and Qin, 1996). Polyethylene oxide used in this study, has been provided by the manufacturer (Aldrich) a melt point of 61.7–66.6 °C and a flash point of >113.0 °C. Therefore, a pyrolysis temperature of 500–600 °C was attained at 10 °C/min and maintained for 2 h in order to decompose CTS/PEO. The nanofibers preserve their morphology and a decrease of 8–40% in size of nanofiber diameters is observed (Supporting Information, Fig. SF-7). Although the regression on the nanofibers of CTS(PEO)/SiO_2 30/70 wt.% ratio corresponds roughly to the organic polymer content, that of 50/50 wt.% ratio represents only a small amount of CTS/PEO showing a little effect of pyrolysis. In this last case, an effective coating of the organic part by the silicate component and an efficient compact structure could protect the core material from decomposing.

3.3. Cell culture and bioactivity

The as-spun nanofibrous membranes were subsequently examined in respect to their cellular compatibility. The fluorescence microscopic images (Fig. 7) show an excellent adherence and spreading of the bone forming 7F2-cells on the nanofiber mats even after a short culture time of 1 day. Despite the different situation on CTS(PEO)/SiO_2 50/50 wt.% mats (cf. left panel Fig. 7a) compared with 30/70 wt.% mats (cf. Fig. 7e), in both cases the 7F2-cells are well attached to the substrate and spread. Stretched cells with well shaped actin fibers and filopodia are visible. This points an immediate initial adherence, a good and fast attachment as well as the absence of cytotoxic substances. After 6 days on both types of nanofibrous membranes fully confluent layers have been grown (right panel Fig. 7b, d and f). It stands for an undisturbed proliferation and a good cytocompatibility, as it is commonly known for titanium, our reference material (cf. Fig. 7c). From this point of view, the chitosan/polyethylene oxide/silica nanofibers are a suitable substrate for growing bone forming cells and might find application in constructing scaffolds for bone tissue engineering.

Bioactive materials establish key biological interactions through surface chemistry at the interface of this material and a tissue (Saravanapavan & Hench, 2001). The living bone-bonding ability of bioactive glasses depends greatly on the formation of biologically active hydroxyapatite (HAP, [$Ca_{10}(PO_4)_6(OH)_2$]) or hydroxycarbonate apatite (HCA) as to their chemical resemblance to human bones. This mineralization process is taking place in contact with physiological fluids or with simulated body fluids (SBF). Among various forms of bioactive materials, nanofibers derived from silicate precursors via sol–gel exhibit the net advantage of large surface area resulting in fast HAP crystal nucleation (Kim et al., 2006). Moreover, the core–shell nanofibers by the use of the biocompatible polymers

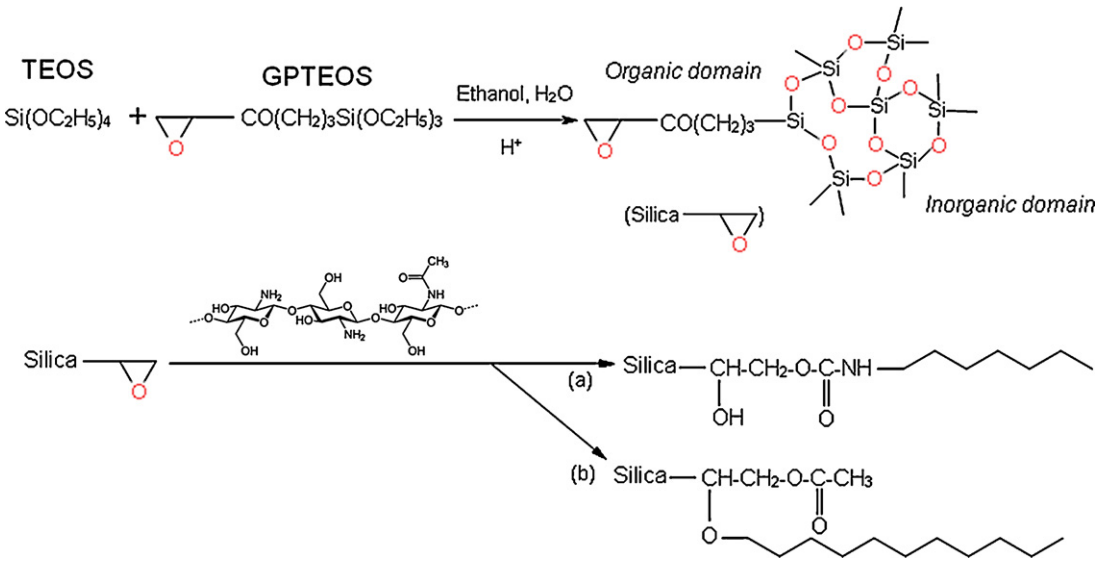

Scheme 1. Potential interactions of the epoxy silica GPTEOS group with chitosan.

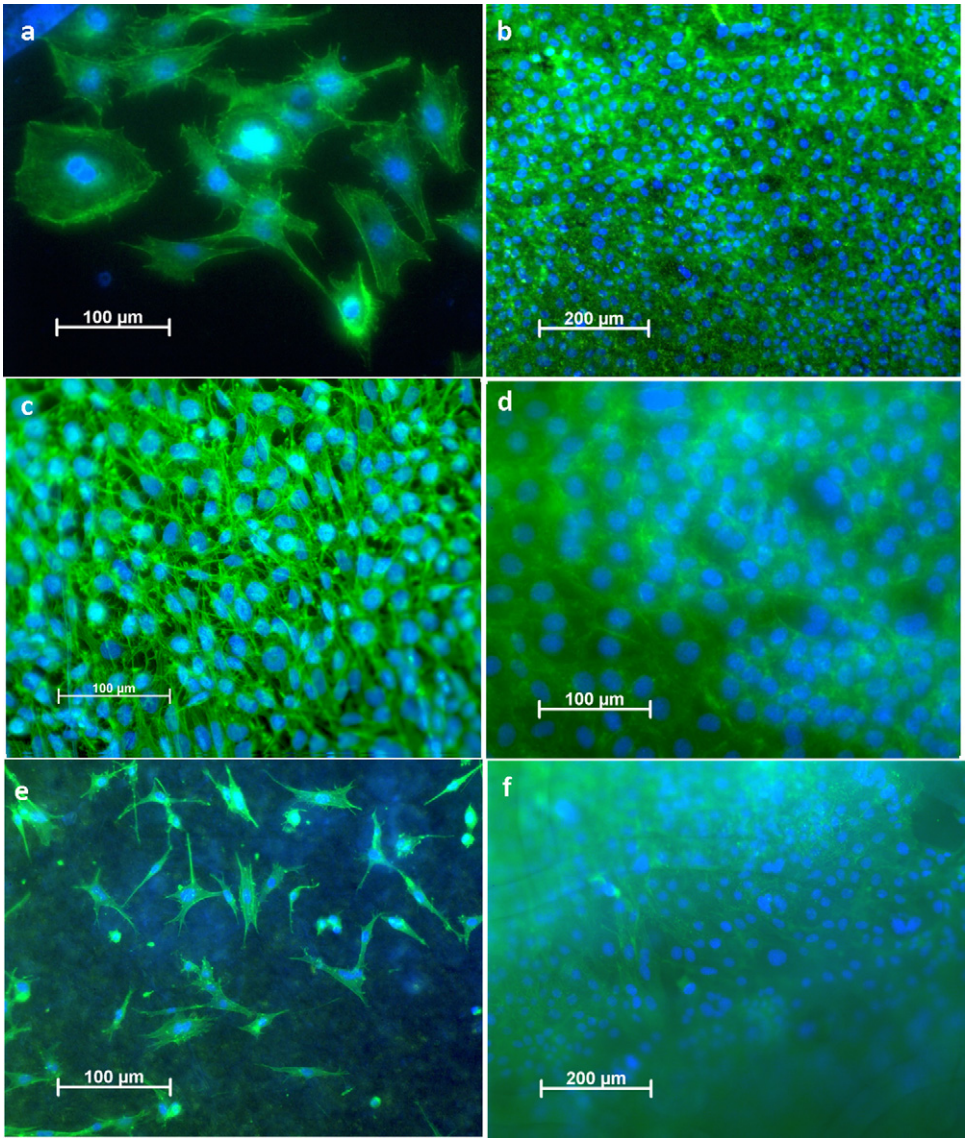

Fig. 7. Fluorescence microscopic images of 7F2-cells on CTS(PEO)/SiO_2 nanofiber mats (a) upper panel left: in a ratio of 50/50 wt.% after 1 day culture time; (b) upper panel right: after 6 days and (d) middle panel right: after 6 days, more detailed image, (c) middle panel left: pure titanium after 3 days as a reference; (e) lower panel left: in a ratio of 30/70 wt.% after 1 day culture time and (f) lower panel right: after 6 days.

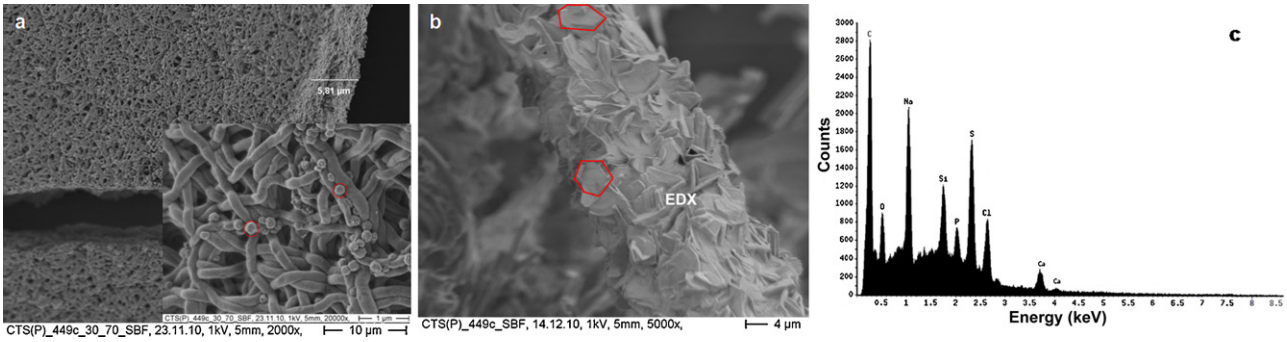

Fig. 8. (a) Effect of CaO as nucleating agent: weak apatite nuclei formation in absence of initially added CaO. (b) Hexagonal 6/m hydroxycarbonate apatite/hydroxyapatite formation on CaO-CTS(PEO)/SiO_2 nanofibers after immersion in m-SBF for 7 days and in (c) EDX spectrum of the hydroxyapatite formation on respective area (b).

CTS/PEO have additional advantages: (i) the inorganic silica component being on the shell/surface of the fiber, thus encapsulating the organic polymer, reacts directly with the SBF solutes, and (ii) they do not require thermal treatment/sintering for the elimination of the polymer, avoiding thus carcinogenesis issues. Certainly, the ability of the silanol groups on silicate ions to act as a nucleation site to form apatite is well known (Cho et al., 1996; Kokubo & Takadama, 2006; Li et al., 1992). From the various types of SBF solutes used in vitro investigations, the modified simulated body fluid, m-SBF has the advantages of containing ion concentrations equal to those of blood plasma and being stable for a long time stored at 5 °C. In our study, the concentration of HCO_3^- is decreased to the level of saturation with respect to the calcite ($CaCO_3$) phase (Oyane et al., 2002). When the as-spun CTS(PEO)/SiO_2 nanofibers were incubated for 7 days in absence of a nucleation initiator, they showed only a small capability in producing spherical apatite (see Fig. 8a). Nonetheless, the nanofibrous non-woven fabric displays an interesting compact 3D structure with a thickness of 5.8 μm and small pores of around 1 μm (see in more detail the Supporting Information, Fig. SF-8). The formation of apatite was greatly favored on nanofibers in which a small amount down to 1.2 wt.% of CaO, in the form of calcium chloride dehydrate, was initially introduced in the sol–gel solution. After immersion and incubation for 7 days at 37 °C, the fibers are covered with a dense layer of sheet-like apatite (see Fig. 8b). In some parts of the coated fibers, one can also observe the initiation of hexagonal 6/m structures characteristic for the apatite crystal nucleation system. Thereby, the crystals observed in Fig. 8b can be attributed to the calcium precipitated as nanocrystalline phase.

The EDX spectroscopy analysis, on a single fiber (Fig. 8c) unveils a high concentration of P on the surface and reveals a Ca/P coating ratio of approximately 1.3, lower to the stoichiometry of hydroxyapatite (Ca/P = 1.67) but closer to that of hydroxycarbonate apatite (Ca/P = 1.5) (Kim et al., 2006; Saravanapavan & Hench, 2001). This ratio determined by semiquantitative EDX analysis is comparable to that of bonelike minerals (Mann, 1988). The silanol groups (Si—OH), present through the sol–gel system induce $Ca_3(PO_4)_2$ nucleation via precipitation of Ca^{2+} and PO_4^{3-} and also CO^{3-}. In addition, carbonate ions have shown to replace the hydroxyl ions in the apatite crystal lattice (Lee, Lu, Baer, Markel, & Murphy, 2010). Furthermore, the presence of the positively charged amine groups of chitosan could reduce the apatite formation ability and lower the Ca/P ratio, through interaction with the negatively charged silica species. This phenomenon was also observed in the case of silica–collagen xerogel (Heinemann et al., 2009).

The major elements detected confirmed the presence of the ions used for the m-SBF composition. Increased carbon (C) content could also result from the sputtering of the pellets to provide the surface conductivity for SEM observation. Silicon (Si) is still present due to the large amount of silanol groups on the nanofiber surface. The observed strong peak of sulfur (S) can be attributed to the large amount (17.892 g L^{-1}) of 2-(4-(2-hydroxyethyl)-1-piperazinyl)ethanesulfonic acid (HEPES), introduced in m-SBF (Oyane et al., 2002).

Hydroxyapatite/silica nanofibers have been found promoting new bone formation when implanted in vivo (Seol et al., 2010). Thereby, the CTS(PEO)/SiO_2 mineralized nanofibrous scaffold could promote new bone formation when implanted in defected sites i.e. for the periodontal tissue reconstruction.

4. Conclusions

Sol–gel derived hybrid silica glass nanofibers containing chitosan (PEO) were fabricated and their structural properties were comprehensively studied. The nanofibers present an enhanced compact structure as confirmed by SEM and TEM measurements. The chitosan fraction in wt.% ratio has been found to influence the length scale of the structure formation, as the CTS(PEO)/SiO_2 50/50 wt.% ratio generating nanofibers with small average diameter of rating 182 ± 16 nm. This tighter chain entanglement might be explained by the strong interaction between the epoxy group of the organosilane GPTEOS used and the amine groups of chitosan chains, triggering covalent bonds. The TEM micrographs revealed nanofibers based on self-assembled core–shell structure. These results have been confirmed by ATR–FTIR analysis, whereas CTS/PEO is encapsulated to form the fibers 'core' coated by the silicate component as shell. The consequence is a fast apatite crystal nucleation when immersed in m-SBF. The as-spun nanofibers were in parallel proved cytocompatible. Cell fluorescence microscopy has shown that nanofiber membranes promote the attachment and proliferation of murine osteoblast-like 7F2-cells. The combination of these hybrid nanofibers made of biocompatible polymers CTS/PEO and silicate facilitate advantages of both materials and offer novel tunable properties for creating bioactive scaffolds for bone repair. Further future investigations will comprise the mechanical properties, biodegradation and inner chemical configuration of various polymer/silica ratios.

Acknowledgements

First author cordially thanks his early Professors at the Université Pierre et Marie Curie, Paris, France: Messrs. Pierre Sigwalt, Jean-Pierre Vairon, Patrick Hemery and Michel Moreau, for teaching him Polymer Science and Ethics. He is also indebted to Emeritus Professors Messrs. Hartmut Worch (Technische Universität Dresden) and Horst Böttcher (Gesellschaft zur Förderung von Medizin-, Bio- und Umwelttechnologien e.V. (GMBU), Dresden, Germany) for their precious encouragement. Authors are also grateful to Dr. Sascha Heinemann of the Max Bergmann Center of Biomaterials Dresden (TUD) for preparation of the substrates for cell

experiments and kind supply of the m-SBF solution. They also thank Mr. Axel Mensch responsible for the SEM laboratory of the Institute of Materials Science of the Technical University of Dresden (TUD) and his collaborators Mrs. Silvia Muehle and Mrs. Ortrud Trommer for their invaluable help; also thank Mrs. Martina Dziewiencki (ITM/TUD) for the FTIR and Mr. Nicolas Cheval (University of Nottingham) for the TEM measurements.

Appendix A. Supplementary data

Supplementary data associated with this article can be found, in the online version, at http://dx.doi.org/10.1016/j.carbpol.2013.01.068.

References

Agboh, O. C., & Qin, Y. (1996). Chitin and chitosan fibres. *Polymers for Advanced Technologies*, *8*, 355–365.

Allo, B. A., Rizkalla, A. S., & Mequanint, K. (2010). Synthesis and electrospinning of ε-polycaprolactone-bioactive glass hybrid biomaterials via a sol–gel process. *Langmuir*, *26*, 18340–18348.

Bhattarai, N., Edmondson, D., Veiseh, O., Matsen, F. A., & Zhang, M. (2005). Electrospun chitosan-based nanofibers and their cellular compatibility. *Biomaterials*, *26*, 6176–6184.

Cho, S. B., Miyaji, F., Kokubo, T., Nakanishi, K., Soga, N., & Nakamura, T. (1996). Apatite-forming ability of silicate ion dissolved from silica gels. *Journal of Biomedical Materials Research*, *32*, 375–381.

Choi, S.-S., Lee, S. G., Im, S. S., Kim, S. H., & Joo, Y. L. (2003). Silica nanofibers from electrospinning/sol–gel process. *Journal of Materials Science Letters*, *22*, 891–893.

Chronakis, I. S., & Ramzi, M. (2002). Isotropic-nematic phase equilibrium and phase separation of κ-carrageenan in aqueous salt solution: Experimental and theoretical approaches. *Biomacromolecules*, *3*, 793–804.

Coradin, T., Durupthy, O., & Livage, J. (2002). Interactions of amino-containing peptides with sodium silicate and colloidal silica: A biomimetic approach of silicification. *Langmuir*, *18*, 2331–2336.

Coradin, T., & Livage, J. (2007). Aqueous silicates in biological sol–gel applications: New perspectives for old precursors. *Accounts of Chemical Research*, *40*, 819–826.

Gaharwar, A. K., Schexnailder, P. J., Jin, Q., Wu, C.-J., & Schmidt, G. (2010). Addition of chitosan to silicate cross-linked PEO for tuning osteoblast cell adhesion and mineralization. *ACS Applied Materials and Interfaces*, *2*, 3119–3127.

Heinemann, S., Heinemann, C., Bernhardt, R., Reinstorf, A., Nies, B., Meyer, M., et al. (2009). Bioactive silica–collagen composite xerogels modified by calcium phosphate phases with adjustable mechanical properties for bone replacement. *Acta Biomaterialia*, *5*, 1979–1990.

Heinemann, S., Coradin, T., Worch, H., Wiesmann, H. P., & Hanke, T. (2011). Possibilities and limitations of preparing silica/collagen/hydroxyapatite composite xerogels as load-bearing biomaterials. *Composites Science Technology*, *71*, 873–1880.

Jun, S. H., Lee, E. J., Yook, S. W., Kim, H. E., Kim, H. W., & Koh, Y. H. (2010). A bioactive coating of a silica xerogel/chitosan hybrid on titanium by a room temperature sol–gel process. *Acta Biomaterialia*, *6*, 302–307.

Kim, H.-W., Kim, H.-E., & Knowles, J. C. (2006). Production and potential of bioactive glass nanofibers as a next-generation biomaterial. *Advanced Functional Materials*, *16*, 1529–1535.

Kim, Y.-J., Ahn, C. H., & Choi, M. O. (2010). Effect of thermal treatment on the characteristics of electrospun PVDF silica composite nanofibrous membrane. *European Polymer Journal*, *46*, 1957–1965.

Klossner, R. R., Queen, H. A., Coughlin, A. J., & Krause, W. E. (2008). Correlation of Chitosan's rheological properties and its ability to electrospin. *Biomacromolecules*, *9*, 2947–2953.

Kokubo, T. (1991). Bioactive glass-ceramics: Properties and applications. *Biomaterials*, *12*, 155–163.

Kokubo, T., & Takadama, H. (2006). How useful is SBF in predicting in vivo bone bioactivity? *Biomaterials*, *27*, 2907–2915.

Lee, J. S., Lu, Y., Baer, G. S., Markel, M. D., & Murphy, W. L. (2010). Controllable protein delivery from coated surgical sutures. *Journal of Materials Chemistry*, *20*, 8894–8903.

Li, P., Ohtsuki, C., Kokubo, T., Nakanishi, K., Soga, N., Nakamura, T., et al. (1992). Apatite formation induced by silica-gel in a simulated body-fluid. *Journal of the American Ceramic Society*, *75*, 2094–2097.

Liu, Y.-L., Su, Y.-H., & Lai, J.-Y. (2004). In situ crosslinking of chitosan and formation of chitosan–silica hybrid membranes with using g-glycidoxypropyltrimethoxysilane as a crosslinking agent. *Polymer*, *45*, 6831–6837.

Liu, Y., Sagi, S., Chandrasekar, R., Zhang, L., Hedin, N. E., & Fong, H. (2008). Preparation and characterization of electrospun SiO_2 nanofibers. *Journal of Nanoscience and Nanotechnology*, *8*, 1528–1536.

Mahltig, B., Fiedler, D., Fischer, A., & Simon, P. (2010). Antimicrobial coatings on textiles-modification of sol–gel layers with organic and inorganic biocides. *Journal of Sol–Gel Science and Technology*, *55*, 269–277.

Mahony, O., Tsigkou, O., Ionescu, C., Minelli, C., Ling, L., Hanly, R., et al. (2010). Silica–gelatin hybrids with tailorable degradation and mechanical properties for tissue regeneration. *Advanced Functional Materials*, *20*, 3835–3845.

Mann, S. (1988). Molecular recognition in biomineralization. *Nature*, *332*, 119–124.

Muzzarelli, R. A. A. (2009). Chitins and chitosans for the repair of wounded skin, nerve, cartilage and bone. *Carbohydrate Polymers*, *76*, 167–182.

Muzzarelli, R. A. A. (2011). Chitosan composites with inorganics, morphogenetic proteins and stem cells, for bone regeneration. *Carbohydrate Polymers*, *83*, 1433–1445.

Ohkawa, K., Cha, D., Kim, H., Nishida, A., & Yamamoto, H. (2004). Electrospinning of chitosan. *Macromolecular Rapid Communications*, *25*(18), 1600–1605.

Oyane, A., Kim, H.-M., Furuya, T., Kokubo, T., Miyazaki, T., & Nakamura, T. (2002). Preparation and assessment of revised simulated body fluids. *Journal of Biomedical Materials Research*, *65*, 188–195.

Poologasundarampillai, G., Ionescu, C., Tsigkou, O., Murugesan, M., Hill, R. G., Stevens, M. M., et al. (2010). Synthesis of bioactive class II poly(g-glutamic acid)/silica hybrids for bone regeneration. *Journal of Materials Chemistry*, *20*, 8952–8961.

Saravanapavan, P., & Hench, L. L. (2001). Low-temperature synthesis, structure, and bioactivity of gel-derived glasses in the binary $CaO–SiO_2$ system. *Journal of Biomedical Materials Research*, *54*, 608–618.

Seol, Y.-J., Kim, K.-H., Kim, I. A., & Rhee, S.-H. (2010). Osteoconductive and degradable electrospun nonwoven poly(e-caprolactone)/$CaO–SiO_2$ gel composite fabric. *Journal of Biomedical Materials Research A*, *94*, 649–659.

Shao, C., Kim, H.-Y., Gong, J., Ding, B., Lee, D.-R., & Park, S.-J. (2003). Fiber mats of poly(vinyl alcohol)/silica composite via electrospinning. *Materials Letters*, *57*, 1579–1584.

Shirosaki, Y., Tsuru, K., Hayaka, S., Osaka, A., Lopes, M. A., Santos, J. D., et al. (2005). In vitro cytocompatibility of MG63 cells on chitosan–organosiloxane hybrid membranes. *Biomaterials*, *26*, 485–493.

Shirosaki, Y., Botelho, C. M., Lopes, M. A., & Santos, J. D. (2009). Synthesis and characterization of chitosan–silicate hydrogel as resorbable vehicle for Bonelike® bone graft. *Journal of Nanoscience and Nanotechnology*, *9*, 3714–3719.

Shirosaki, Y., Tsuru, K., Satoshi Hayakawa, S., Osaka, A., Lopes, M. A., Santos, J. D., et al. (2009). Physical, chemical and in vitro biological profile of chitosan hybrid membrane as a function of organosiloxane concentration. *Acta Biomaterialia*, *5*, 346–355.

Spirk, S., Findenig, G., Doliska, A., Reichel, V. E., Swanson, N. L., Kargl, R., et al. (2012). Chitosan–silane sol–gel hybrid thin films with controllable layer thickness and morphology. *Carbohydrate Polymers*, http://dx.doi.org/10.1016/j.carbpol.2012.04.030

Sridhar, R., Sundarrajan, S., Venugopal, J. R., Ravichandran, R., & Ramakrishna, S. (2012). Electrospun inorganic and polymer composite nanofibers for biomedical applications, Journal of Biomaterials Science. *Polymer Edition*, 1–21.

Suzuki, T., & Mizushima, Y. (1997). Characteristics of silica–chitosan complex membrane and their relationships to the characteristics of growth and adhesiveness of L-929 cells cultured on the biomembrane. *Journal of Fermentation and Bioengineering*, *84*, 128–132.

Tian, D., Dubois, P. H., Grandfils, C. H., Jérôme, P., Viville, P., & Lazzaroni, R. (1997). A novel biodegradable and biocompatible ceramer prepared by the sol–gel process. *Chemistry of Materials*, *9*, 871–874.

Toskas, G., Laourine, E., Kaeosombon, W., & Cherif, C. (2009). Electrospinning of collagen and chitosan in perspective of medical scaffolds applications. In *International conference on latest advancements in high tech textiles and textile-based materials* Gent, Belgium,

Toskas, G., Hund, R. D., Laourine, E., Cherif, C., Smyrniotopoulos, V., & Roussis, V. (2011). Nanofibers based on polysaccharides from the green seaweed Ulva Rigida. *Carbohydrate Polymers*, *84*, 1093–1102.

Toskas, G., Cherif, C., Hund, R. D., Laourine, E., Fahmi, A., & Mahltig, B. (2011). Inorganic/organic (SiO_2)/PEO hybrid electrospun nanofibers produced from a modified sol- and their surface modification possibilities. *ACS Applied Materials and Interfaces*, *3*, 3673–3681.

Toskas, G., Hund, R.-D., Laourine, E., & Cherif, C. (2012). Nanofibers from natural biopolymers in regenerative medicine. In A. El Nemr (Ed.), *Textiles: Types, uses and production methods* (pp. 203–221). New York: Nova Science Publishers.

Wei, M., Lee, J., Kang, B., & Mead, J. (2005). Preparation of core–sheath nanofibers from conducting polymer blends. *Macromolecular Rapid Communications*, *26*, 1127–1132.

Zhang, J.-F., Yang, D.-Z., Xu, F., Zhang, Z.-P., Yin, R.-X., & Nie, J. (2009). Electrospun core–shell structure nanofibers from homogeneous solution of poly(ethylene oxide)/chitosan. *Macromolecules*, *42*, 5278–5284.